physica status solidi
pss
www.pss-journals.com

reprint

WILEY-VCH

Phys. Status Solidi B **249**, No. 4, 644–652 (2012) / **DOI** 10.1002/pssb.201100805

physica status solidi b
www.pss-b.com
basic solid state physics

Feature Article

Electroluminescence properties of organic nanostructures studied by scanning tunnelling microscopy

Klaus Kuhnke[*,1], **Alexander Kabakchiev**[1], **Theresa Lutz**[1], **and Klaus Kern**[1,2]

[1] Max-Planck Institute for Solid State Research, Heisenbergstrasse 1, 70169 Stuttgart, Germany
[2] Institut de Physique des Nanostructures, Ecole Politechnique Fédérale de Lausanne, 1015 Lausanne, Switzerland

Received 1 December 2011, revised 7 January 2012, accepted 13 January 2012

Keywords luminescence, pentacene, photon time-correlation, scanning tunnelling microscopy

---

[*] Corresponding author: e-mail k.kuhnke@fkf.mpg.de, Phone: +49 711 689 1454, Fax: +49 711 689 1079

The control of light emission on the scale of individual quantum systems, like molecules or quantum dots, is a field of intense current research. One way to induce light emission from these systems is the local charge injection through the tip of a scanning tunnelling microscope (STM). Studies which employ this method have to address one basic question: Does the detected luminescence provide information precisely from the molecule into which charge is injected by the STM tip apex or are the luminescence properties determined by a larger volume? In this article, we focus on the investigation of organic nanocrystals and discuss the relation between the local excitation, the intermolecular coupling and the influence of the STM as a measuring instrument. Choosing pentacene as an organic emitter, we present results, which suggest that the STM-induced luminescence cannot be attributed simply to the emission by a single molecule. We discuss how information about locality can be obtained and comment on the present experimental limitations and possible future improvements.

1 Introduction

Individual nanometer structures with well-defined electronic states can be employed as light sources with unique luminescence properties [1]. Applications can aim at the generation of entangled photon pairs or the emission of single photons on demand [2]. One choice for nanostructures, which can provide photons of designable properties are semiconductor quantum dots as discussed in a number of contributions in this journal issue. One may find more "natural" representatives of quantum systems with similar properties by choosing appropriate luminescent molecules with spatially extended electronic π-systems. Thin films composed of such molecules are also of significant interest with regard to their properties as organic semiconductors in the perspective of organic electronic conductors, transistors [3], or organic light emitting diodes (OLEDs) [4]. The luminescence from thin organic layers can be studied by scanning tunnelling microscopy (STM) when the set-up is extended by an optical detection system (Fig. 1). Light originating from the tunnel junction is focussed on a photon counter or spectrometer entrance slit. It is possible to detect and analyze the luminescence outside an ultra-high vacuum (UHV) chamber without rise of the sample temperature inside a liquid helium cryostat (4.2 K) [5].

In the combination with light detection, electron tunnelling microscopy and spectroscopy are employed to gain spatially resolved information on the structure and electronic states of the investigated sample. The optical part of the set-up allows recording spectra and total intensity of

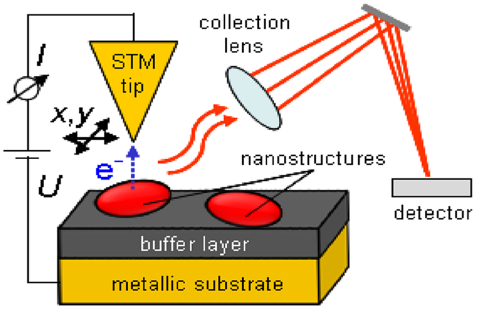

Figure 1 (online colour at: www.pss-b.com) Schematic illustration of STM on nanostructures extended by luminescence detection.

the luminescence induced by the tunnel current. Both can be recorded as a function of the STM tip position. The optical access opens in addition the possibility to measure nanosecond-scale photon time correlations, which will be discussed in detail below.

Light emission from the tunnelling junction of an STM has first been explored and its mechanisms elucidated through a number of pioneering publications [6–9]. Changes of the tunnel current induced luminescence have been resolved with a lateral resolution close to the atomic scale on various surfaces [10–14]. The luminescence on a clean metal sample was identified to be due to inelastic tunnelling [15] between metal and sample. The process results in a wide spectral light distribution, which reflects the plasmonic cavity modes between the two metal contacts [9, 16, 17]. STM-induced luminescence (STL) has moreover been applied to study surfaces of inorganic bulk semiconductors [18–20] providing local information of electron–hole recombination. Within the last decade luminescence detection became a more widely applied extension to STM for the characterization of semiconductors and due to an increasing interest in the luminescence from organic substances. The successful demonstration of luminescence from an individual molecule on an ultrathin insulating film [21] brought its potential to wide attention. This achievement suggests the perspective to chemically identify molecules and to study their properties and intramolecular processes by means of their luminescence. Up to date, the intrinsic luminescence of isolated molecules on an ultrathin oxide layer has been exploited extensively only for one class of compounds (Zn(II)-etioporphyrin I [21], Mg-porphine [22, 23]). In an alternative approach, molecular films have been studied, starting from experiments on monolayers [24] and extending to nanocrystals [25, 26] and ultrathin films of systematically varied thickness [27, 28]. Such investigations are a successful path to obtain STM-induced chemically specific luminescence. The strong point of STM, to image individual electronic orbitals even on thick molecular films [29, 30] suggests that this ability to access local properties should be transferable to luminescence experiments. After all, the emitted light originates from the recombination of electron–hole pairs, which populate the imaged orbitals. However, this concept competes with intermolecular coupling mechanisms. They induce electronic band formation long before bulk dimensions are reached and are since long known to yield also excitonic bands [31].

The interest in luminescence and transport properties of organic films provides an additional motivation to investigate the possibility that local charge injection may address one molecule below the tip apex and read out its individual optical properties. Comparing the thin film studies to the ones on isolated molecules, it is of interest to discuss the issue, to which degree the luminescence is affected by the coupling to neighbouring molecules and to which degree it may retain single molecule properties. This question will be at the focus of this article. We will base the discussion on experimental data from individual pentacene (Pc) nanocrystals and other results from the literature. For a more extensive and general discussion of topics in scanning-tunneling-microscopy-induced light emission, we would like to refer the reader to a recent review [32]. We remark that the experimental method has not yet been assigned a unique acronym, which makes literature search more tedious. In most publications (as also in this one), no specific acronym is employed as a keyword. In the text of this article, we will use "STL" (STM-induced luminescence) for brevity while by other authors "STM-LE" (STM-induced light emission) is used in perfectly the same context.

This feature article is organized as follows: In Section 2, we briefly discuss the basic mechanisms of STM-induced luminescence on molecular systems. In addition, we introduce experimental methods, which allow to access properties, which cannot be studied by mere electron tunneling spectroscopy. Section 3 presents the luminescence spectra obtained from Pc nanocrystals. The origin of the luminescence is discussed in comparison to photoluminescence studies on different Pc samples. While Section 3 deals with the spectroscopic information on the molecular environment, Section 4 will address instrumental effects on the observed luminescence spectra. STM affects the measurements by the proximity of metallic electrodes and by the strong electric field in the tunnel gap. Section 5 presents a photon–photon time correlation measurement on a Pc nanocrystal and discusses the conclusions, which have to be drawn from the fact that no photon anti-correlation could be observed. Section 6 gathers results from Sections 3–5 and other publications in order to discuss properties of intrinsic STM-induced luminescence. Section 7 concludes the article and gives an outlook on possible future developments.

2 STM-induced electroluminescence (STL) The emission of light from a metallic STM tip in tunnel contact to a metal substrate is due to tip-induced surface plasmons [16]. These plasmonic cavity modes are localized between the curved tip and the flat substrate [33] and can be excited by the statistical fluctuations in the tunnel current [34]. The cavity modes efficiently couple to the electromagnetic far field into which the energy can eventually be radiated as photons [35]. This coupling is related to the electromagnetic field enhancement at sharp tips. Depositing a single layer of molecules on the metallic substrate typically changes the luminescence spectrum. In addition, the total emitted intensity may either increase or decrease [36]. The role of intramolecular electronic transitions in the emission from the plasmonic cavity modes has still to be clarified in detail. However, it has been established that an increasing film thickness leads to a continuous transition from the spectrally broad plasmonic emission to a narrow intrinsic emission line [27]. This observation demonstrates that a few layers of the organic molecule can serve as a buffer, which decouples organic molecules from the metallic substrate. The increased distance between tip and metallic substrate, which results from the introduction of the organic layer typically reduces the direct excitation of broadband plasmonic emission [37] although exceptions have been reported [38]. Nevertheless, also for the intrinsic molecular luminescence, the plasmonic cavity modes were found to play a decisive role in coupling the local molecular luminescence to the detected electromagnetic far field [26]. A comparison between luminescence spectra obtained for different tip and substrate materials suggests that Ag tips provide a strong increase in the detectable intensity. Spectral regions can be boosted or attenuated by selecting substrate and tip metals and by modification of the tip shape [21, 31, 39–41].

In Fig. 2, we sketch the energy levels of a generic quantum system in a STM junction. The quantum system may for instance be a molecule or a quantum dot. We assume that it is decoupled from the metallic substrate by a thin insulator or wide band gap semiconductor. Plasmonic emission can be generated in this system by direct inelastic tunnelling from the occupied states of the substrate into the unoccupied states in the tip. The range of available energies for initial and final states provides a wide spectral distribution of emitted light. With increasing tunnelling distance between tip and substrate this contribution typically decreases. The electronic transition (marked in orange) between two levels within the quantum system will generate energetically narrow emission (orange wave), which corresponds to a sharp line in the luminescence spectrum. From the energy level diagram, it is obvious that the emission of intrinsic luminescence requires the existence of two states in the quantum system at energies between the tip and the substrate Fermi energies. Moreover, the higher energy state must be at least partially occupied while the lower state must be at least partially unoccupied. The latter is the more crucial point and requires that the tunnel rate towards the tip becomes large enough to compensate for the refilling by tunnelling or even conduction from the substrate. For small tunnel currents in the pA range, the vacuum tunnel barrier is typically rate limiting in comparison to the barrier by an ultrathin semiconductor or insulator. Charge tunnelling through the vacuum to a given state is more efficient, the closer the state is situated to the vacuum level. Intrinsic luminescence at negative bias, as sketched in Fig. 2, requires vacuum tunnelling out of a low-lying state. In contrast, a positive bias voltage would allow tunnelling through the vacuum into a higher-lying state. Based on the asymmetry of vacuum and buffer barrier, this argument suggests that a positive bias voltage may be favourable for the generation of intrinsic luminescence [21–23, 42]. While films of porphyrins have been reported to luminesce at positive and negative bias (bipolar luminescence) [28, 43], it is remarkable, that for other molecules intrinsic luminescence could only be observed at negative bias [25, 29]. The latter applies also to Pc, which is discussed in more detail below.

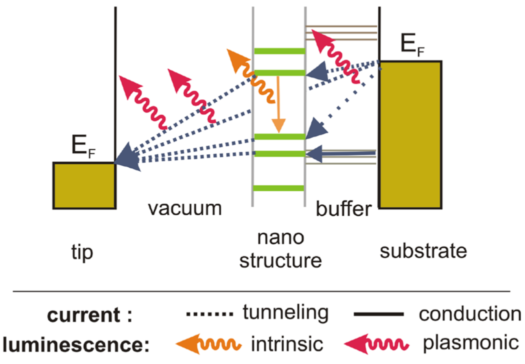

Figure 2 (online colour at: www.pss-b.com) Energy level diagram for electron transitions through a nanostructure between two tunnel contacts (vacuum and buffer layer) at negative bias of the substrate with respect to the tip. Inelastic tunnelling paths can provide plasmonic luminescence. Only the vertical (orange) transition within the nanostructure leads to intrinsic luminescence.

There are other channels to electroluminescence in the STM, which involve on one side a discrete level of the quantum system and on the other side a metal electrode, either tip or substrate. These transitions were tagged by red wavy arrows in Fig. 2 in the same way as the tunneling from metal-to-metal. They can generate strong and spectrally broad luminescence, which may in experiment render the intrinsic luminescence (orange wave) unobservable.

As already pointed out, the intrinsic luminescence depends on the transition between two discrete levels between the Fermi energies of tip and substrate. In a semiconductor-like picture, this process corresponds to the recombination of an electron and a hole injected from opposite sides by the two electrodes. Prior to recombination the opposite charges will typically bind to each other through electrostatic interaction and form an exciton at a reduced total energy. Due to this interaction, the study of radiatively decaying electron–hole pairs or excitons goes beyond the separate characterization of electron and hole states. At this point, STM-induced luminescence can provide information, which is inaccessible to scanning tunnelling (electron) spectroscopy. Still other properties become accessible through photon–photon time correlation measurements [44, 45]. They can provide valuable information by testing if the observed luminescence is due to the emission of an individual quantum system even if the source cannot be resolved microscopically [46]. The photon correlation technique has already been employed in STM-induced luminescence [47]. A positive STM-based proof of single molecule emission has, however, not yet been reported. For an adsorbate layer in solution, the bunched emission of photons has been observed [48]. The observation was attributed to a change between higher and lower luminescence intensity correlated with the diffusion of molecules below the STM tip. In Chapter 5, we will discuss a photon correlation measurement on a Pc nanocrystal at 4.2 K. There, the implications of employing photon–photon correlations in the environment of the STM tunnel junction will be discussed in detail.

3 STL from Pc nanocrystals

In organic electronics, Pc is not regarded as an efficient luminescent substance in the first place. As we will discuss in more detail below, the fission of the free singlet exciton to two non-radiative triplet excitons at about half of its energy may reduce its luminescence. Pc is rather known as a semiconductor with high carrier mobility [49].

However, Pc has the advantage that its structural, electronic and optical properties have been determined in a significant number of experimental and theoretical studies. We prepared in UHV Pc nanocrystals on an ultrathin KCl layer on top of low index single crystal surfaces (Au(111), Ag(111), Cu(111)). The Pc molecules arrange in a structure, which corresponds to its bulk structure [50] within the experimental precision of STM topography. The height of a molecular layer is 0.3 nm. The nanocrystals typically form a truncated step-pyramid shape as exemplified by the topographic image in Fig. 3. A sharp STM tip allows imaging steps of single (0.3 nm) or double (0.6 nm) layer height near the edges of the crystals.

It can be excluded that the first layer consists of upright standing molecules (1.5 nm height) because crystal regions and whole crystals lower than 1 nm are observed. Moreover, the molecular L-axis (Fig. 3a) of the imaged molecules is always found to be parallel to the surface plane (Fig. 3b). This contrasts to the molecular orientation of Pc on other insulators [51–54]. The layered structure and the high crystal quality suggest that grain boundaries do not play a role in the vertical charge transport in the STM. Details of the preparation and structure parameters of the Pc nanocrystals have been presented in detail in a previous publication [29].

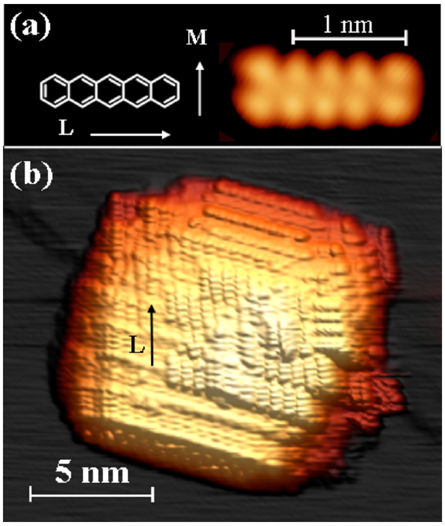

Figure 3 (online colour at: www.pss-b.com) (a) Left: Chemical structure of Pc with arrows defining the long (L) and the intermediate (M) molecular axis. Right: HOMO orbital of an individual molecule imaged by STM (bias −2.2 V, current 75 pA). (b) Topograph of a nanocrystal of 1.5 nm height illustrating the crystalline layered shape and the orientation of the molecular L-axis parallel to the surface plane. The colour represents the height information; in addition a shadow-casting light source is employed to enhance the molecular features (bias voltage: −3.0 V, current: 20 pA).

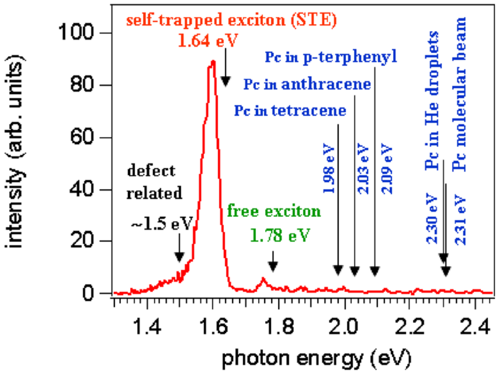

Figure 4 (online colour at: www.pss-b.com) STM-induced electroluminescence spectrum of a Pc nanocrystal (height 1.8 nm). The spectrum has been accumulated for 100 s at −2.6 V bias voltage and 1 nA current. The arrows indicate transition energies of single exciton decay from different publications (see text).

Figure 4 shows a typical STM-induced electroluminescence spectrum recorded on a Pc nanocrystal. An intense line is observed at 1.59 eV, a weak shoulder around 1.5 eV and a very weak but sharp peak at 1.76 eV. No plasmonic background is observed in the spectrum, indicating that the emission is exclusively induced by molecular transitions and not by the broadband fluctuations in the tunnel current. The arrows in Fig. 4 mark emission energies of the lowest singlet exciton measured by photoluminescence studies: Free single Pc molecules exhibit a transition at 2.30 eV (molecular beam [55]) and 2.31 eV (Pc in He droplets [56]). Molecules embedded in organic matrices have emission energies between 2.0 and 2.1 eV [57–59]. Finally, the photoluminescence from macroscopic crystals grown from purified Pc [60] exhibits three lines at ~1.5, 1.64 and 1.78 eV. With respect to the 4 K photoluminescence spectrum in that study, we find a striking resemblance to our spectrum, except that the lines of the nanocrystals are red-shifted by a few hundredth of an eV. The resemblance appears even more surprising as the same research group, which studied the crystals, reports measurements on Pc thin films and clusters in which the dominant transition at 1.64 eV is not observed [61]. That line which is situated approximately 0.15 eV below the free singlet exciton has been attributed to a self-trapped exciton [60, 62]. In the Pc crystal the relative intensity shifts from the free to the self-trapped exciton with decreasing temperature [60]. An alternative assignment of the strong transition may be derived from a time-resolved absorption study [63]. The authors of that study present a model in which the free exciton relaxes to an excimer state. With this energy reduction of 0.25 eV a fission of the excimer into two triplet excitons becomes impossible without thermal activation. This mechanism can explain why at low temperature the transition at the reduced energy becomes the strongest feature. Its lineshape is non-Lorentzian, which suggests that it is not determined by lifetime but is rather due to inhomogeneous broadening. The shoulder at 1.5 eV was suggested to result from impurities and defects [60]. On our nanocrystals, the shoulder is invariably observed together with the transition at 1.59 eV, which may also suggest an assignment to a vibrational progression of this transition. The

STL spectra were not found to exhibit additional peaks for increasing tunnel current. There is thus no indication of significant multiple exciton generation, which is in agreement with the analysis of the photon correlation data discussed in Section 5.

The major difference between the discussed study on single crystals in the literature and our experiment is the crystal dimension. We analyzed the effect of the reduced crystal size on the emission spectrum. Exciton confinement in a nanostructure can provide a shift of the emission energy, which could be clearly resolved by STL on individual CdSe quantum wires [64]. The evaluation of Pc spectra from a large number of studied nanocrystals, however, provides no correlation between peak energy and nanocrystal dimension within experimental precision. The exclusive emission from molecules at the crystal surface would result in a blue shift due to the reduced number of neighbours compared to the bulk. This tendency is, however, in the opposite direction as the observed red shift with respect to the macroscopic crystals. Moreover, the surface shift is known to be larger for lying-down molecules than for upright molecules [65].

Individual Pc molecules dispersed on the ultrathin KCl layer were not observed to generate intrinsic luminescence that might emerge within an intense and broad plasmonic background. This observation is in contrast to the studies of porphyrins on an aluminum oxide buffer on NiAl(110) [21–23] but similar to the results for fullerenes on a NaCl buffer on Au(111) [25]. The reason can be the different electronic and optical properties of the different buffer layers and substrate metals. For Pc, another mechanism may contribute: The transition dipole of the lowest singlet exciton is parallel to the molecule's intermediate axis M (see Fig. 3a). As single Pc molecules are adsorbed flat on the insulator layer, the dipole cannot efficiently couple to the cavity plasmons whose electric field direction is perpendicular to the surface. When the molecule is part of a crystal, the transition dipole exhibits a significant component along the surface normal due to the molecule's rotation around the long axis L by approximately 26° [29].

4 Energy shift in the tunnel junction

The environment of the emitting excitonic state is not only defined by the molecular neighbourhood as discussed in Section 3. In fact, another important difference between the photoluminescence study [60] and our set-up is the proximity of the metal electrodes. The screening by metal surfaces can reduce the oscillator frequency at short distance. We estimate that this interaction may yield a red shift in the meV range. The calculation of a reliable value would, however, require a precise knowledge of the transition dipole moment (or the pure radiative life time) and the distance of the exciton emission from tip and substrate.

A clear quantitative dependence is, however, found with respect to the applied bias voltage: A red shift of 15 meV can be attributed to the Stark shift in the electric field between STM tip and substrate. A detailed analysis based on a quadratic Stark shift provides additional information on the excitonic properties. The coefficient of the quadratic term yields the polarizability change $\Delta\alpha$ in the transition from the excitonic state to the ground state. We obtain a value of $\Delta\alpha = 1080\,A^3$ which can be interpreted by a comparison to the molecular volume [66]. The structure parameters yield a volume of $350\,A^3$ per molecule in the bulk [50, 67]. However, the volume of a Pc molecule must be smaller than the space, which it occupies inside the crystal. The fact that $\Delta\alpha$ is three times larger than the molecular volume is a strong indication that the exciton is not localized on a single Pc molecule but is distributed over several molecular sites. Due to this spatial separation, the electric field can easily induce a large dipole moment, which leads to the observed large energy shift. The detailed analysis of these data will be presented in a forthcoming publication [68].

5 Photon–photon time correlation

We now address statistical properties of the light emitted by the nanocrystals. The emission of luminescence by a single molecule (as opposed to an ensemble) can be identified by the statistical analysis of photon emission intervals. We carried out photon–photon time correlation measurements using a gold tip and a Au(111) substrate. As the Pc emission spectrum is dominated by one line (Fig. 4) no spectral discrimination of the light in front of the detectors is required. The experimental set-up is sketched in Fig. 5. The light emission from the tunnel junction is monitored from two orthogonal directions [5]. The third optical path of the set-up remains available for spectroscopy. The photons are detected by two single photon counting avalanche photo diodes (APDs) [69]. The start–stop intervals between

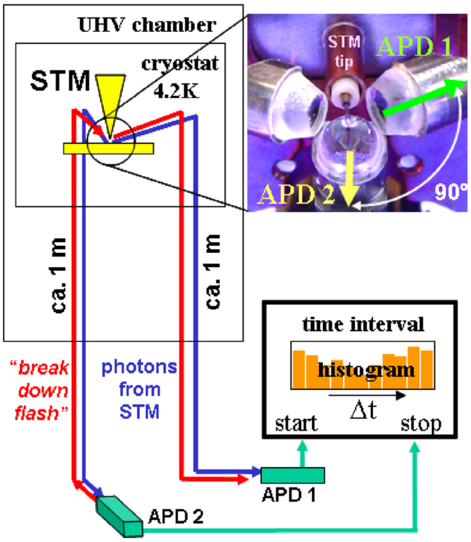

Figure 5 (online colour at: www.pss-b.com) Schematic drawing of the time correlation experiment. The APDs are situated at room temperature outside the UHV chamber and are coupled to two of the optical paths from the tunnel junction. The photograph (top right) shows a close-up view of the STM tip with lenses adjusted to collect the light from the tunnel junction along three orthogonal directions. In the photograph, the sample had been removed.

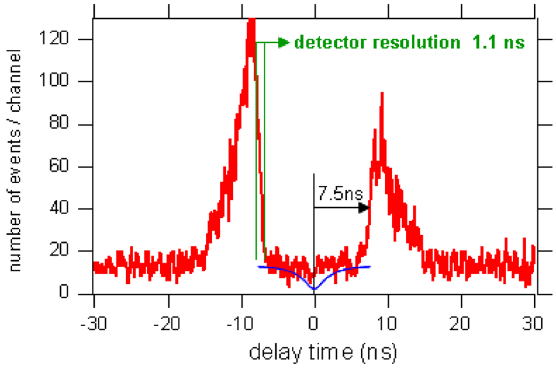

Figure 6 (online colour at: www.pss-b.com) Photon time correlation measurement (red trace) recorded on a 3.0 nm high Pc nanocrystal. The blue trace is a transient simulated for an assumed exciton lifetime of 2 ns.

detected photons are recorded using a time-correlation single photon counting PC card [70]. At -3.3 V bias voltage and 1 nA tunnel current a count rate of the order of 2000 counts/s per APD is obtainable. The red trace in Fig. 6 displays the number of times a certain start–stop time difference was observed during a total accumulation time of 9.6 h. The delay-time-independent number of events per channel due to stochastic coincidences can be obtained by

$$n = \nu_1 \, \nu_2 \, \Delta\tau \, T_{\mathrm{meas}} \tag{1}$$

wherein ν_1 and ν_2 are the counting rates of the APDs, $\Delta\tau$ is the channel width of the correlation measurement (0.18 ns) and T_{meas} is the total accumulation time. The measured 13 events/channel agree well with a long time average of 1500 counts/s per APD. The dark count rate of the detectors is 70 counts/s. It generates events, which are not due to real photons. Employing Eq. 1, it can be estimated that 0.7 spurious events per channel will thus occur.

The histogram in Fig. 6 shows two broad positive correlation features, which are artefacts of the optical set-up. As the observation directions in the STM are orthogonal with respect to each other, the direct optical coupling between the two detectors is extremely small. Each detector has, however, a finite probability to detect a photon emitted by the other detector during an avalanche event. Thus, two artefacts appear which follow the known transient of breakdown luminescence of APDs [71]. The length of the optical path from one detector to the STM tip and back to the other detector (Fig. 5), accounts for the observed delay of ± 7.5 ns (Fig. 6). The artefacts provide two important parameters of the experiment. (1) The delay time-zero is located exactly in the middle between the two features. (2) The fast edge of the artefacts provides an upper limit of 1.1 ns (FWHM) for the experimental time resolution.

Anticorrelations in photon statistics are due to the collapse of the quantum mechanic transition wave function to the emitters' ground state when a luminescence photon is emitted. At this instant, the probability of the emission of another photon becomes exactly zero. This nulls the probability to observe small start–stop time intervals in the correlation function. The probability to emit the next photon recovers within a characteristic time of the system. If the light emission is due to an ensemble of emitters which individualy cycle between ground state and excited state in an uncorrelated manner, the anticorrelation feature is unobservable. It may, however, also become unobservable for a single emitter if the characteristic time of the system is significantly shorter than the time resolution of the experiment. The characteristic time is approximately the minimum of repopulation time and exciton lifetime. The low photon count rate in the experiment suggests a slow repopulation on the microsecond time scale even when we take into account that a significant percentage of the radiated photons remain undetected. This means that the characteristic time of the anticorrelation feature will be dominated by the exciton lifetime.

The lifetime of the lowest singlet state of matrix isolated Pc is of the order of tens of nanoseconds [44]. The non-Lorentzian shape of the transition and its width (Fig. 4) suggest that the lifetime in the experiment must be much longer than 100 fs. A reasonable estimate for the nanocrystal is obtained from transient absorption spectroscopy of microcrystalline bulk Pc. The measured bleaching time of the lowest transition is 0.85 ns [72] and the lifetime of a trapped and relaxed state has been estimated within a model adapted to time resolved measurements as 1.2 ns [63]. These values have been derived from room temperature data. We thus expect that our low temperature time correlation experiment will allow observing a photon anticorrelation minimum if the luminescence is exclusively due to one single emitter.

The experimental signature of photon anticorrelation is a minimum of events at the time zero. The minimum value is given by the number of spurious events (here 0.7 events/channel). The blue curve in Fig. 6 is a simulation assuming an exciton lifetime of 2 ns and a time resolution of 1.1 ns. However, no such anticorrelation feature appears in the data (red curve) although the statistical noise would allow its identification.

As the measurement employs an STM set-up, two contributions may lead to a further reduction of the exciton lifetime. At a tunnel current of 1 nA the nanocrystal is traversed by an electron every 0.16 ns on average. The changing electric field may increase the rate of non-radiative quenching of the exciton. In the experiment, we can rule out this effect because the mechanism would be detectable through a saturation of emission. Figure 7 demonstrates that the luminescence increases linearly at least up to a current of 0.75 nA and no indication of a beginning saturation is observable.

A second possible lifetime reduction may be induced by non-radiative quenching due to the proximity of metal substrate and STM tip. Time resolved experiments and theoretical results suggest that the life time of an emitting state may become shorter than 1 ns at distances from the

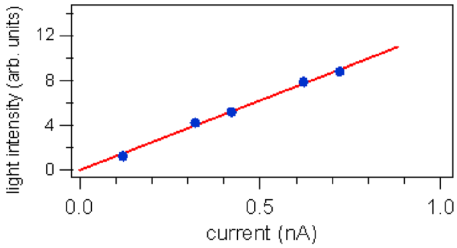

Figure 7 (online colour at: www.pss-b.com) Spectrally integrated electroluminescence from a Pc nanocrystal as a function of tunnel current at −2.6 V bias voltage.

metal below 3 nm [73–75]. Without further investigations, we can thus not exclude that the presence of substrate and tip may prohibit the observation of the photon anti-correlation. A clarifying experiment might be realized by employing semiconducting materials for tip and substrate. While the quenching of the exciton will thus be reduced, the missing plasmonic enhancement [35] will, however, grossly reduce the detectable light intensity. Given the fact that the required accumulation time of the correlation measurement scales with the inverse square of detector count rate (Eq. 1), the modified experiment may not be able to generate sufficient statistics.

6 Discussion

We reported experiments on the luminescence properties of Pc nanocrystals. The crystals are electronically decoupled from a metal substrate by an ultrathin insulator. The observed light emission is exclusively due to narrow intrinsic luminescence while broad plasmonic contributions do not play a role. For this model system, experiments are presented which address different properties of the observed exciton luminescence. The strong influence of the bulk environment on the excitation is evident from the close agreement to single crystal photoluminescence spectra and the clear differences to spectra of matrix embedded molecules. This indicates an emission from sites inside the crystal rather than from its surface. In Section 5, the possible quenching of excitation by the metallic electrodes has been discussed. The efficiency of non-radiative quenching decreases with the third (gold) or fourth (silver) power [75] of the distance from the metal surfaces (tip and substrate). We may thus speculate that only a thin layer of molecules at some depth inside the nanocrystal may efficiently emit luminescence.

The large Stark shift observed for the emission line is not compatible with a localization of both, electron and hole of the exciton on one single Pc molecule. A similar conclusion has been drawn from STL spectra on C_{60} nanocrystals for which the strongest emission line has been assigned to a dimer-related state [32].

Finally, an anti-bunching of luminescence photons is not observed in the luminescence of Pc nanocrystals. This result is compatible with the assumption that several molecules or sites emit luminescence independently from each other. Moreover, the non-Lorentzian lineshape of the transition indicates an inhomogeneous broadening, which may also be due to the emission from different sites. The Davydov splitting which has be identified in the optical constants of Pc [76] might provide another test for the locality of the observed luminescence. As the splitting is due to the presence of two molecules in the unit cell of crystalline Pc, its observation would support the picture of a delocalized emission. Within the above-discussed STL measurements a distinction of the absence or presence of the splitting is, however, not achieved.

The spatial diffusion of excitation, which may lead to delocalization could not be accessed in the experiments on homogeneous Pc nanocrystals. It has, however, been reported for fullerene nanocrystals [32]. In that study, a superposition of two distinct emission spectra at the boundary between C_{60} and C_{70} regions has been reported. The superposition is observed already at a distance of several lattice constants from the topographically sharp boundary. The observation has been attributed to an exciton transfer to nearby molecules with an enhanced efficiency due to the plasmonic cavity modes. While this observation is based on excitation transfer between molecules with different transition energies, one might expect that the coupling will be even stronger for a transfer between identical molecules in a homogeneous layer. This suggests a picture in which excitons and plasmons form combined states. The effects of back coupling of plasmon cavity modes to the molecular emission has recently been treated theoretically [77].

The experimental results obtained by STL consistently suggest that the source of luminescence in the Pc nanocrystals is not one individual molecule below the STM tip. The results reflect different aspects of the delocalization of the luminescence source. In its crystalline structure, Pc exhibits an intermolecular electronic coupling, which is strong in comparison to other organic semiconductors [78]. However, the results will be relevant in general for organic multilayer structures. The distinction between the size of features resolved in the luminescence and the size of the light-emitting source appears non-trivial. Electronic contributions like orbital shapes and the local variation of tunneling conditions have to be distinguished from the extension of the area over which light is emitted.

7 Conclusion and outlook

STM-induced electroluminescence is a technique, which combines luminescence spectroscopy with high-resolution topographic and electronic characterization. For organic nanostructures the method provides a unique probe to investigate electronic transitions. It can access information of excitons, which are two-particle states and are not directly accessible to electron tunneling spectroscopy. Moreover, the detection of luminescence can yield a high sensitivity to the molecular environment. Finally, it is possible to monitor processes on a short time scale, which is not typically reached in tunneling spectroscopy. Based on experiments on Pc nanocrystals, we can state that STL experiments of ultrathin structures are able to identify luminescence properties, which differ from those of isolated molecules.

Future experiments may continue exploring a larger set of organic molecules to make use of the potentially wide applicability of the method. New compounds may improve luminescence efficiency by control of the orientation of the transition dipole moment and the relative population of singlet and triplet states. In electroluminescence devices, 75% of the electron–hole pairs form a typically long-lived and non-radiative triplet state, which reduces the efficiency of light emission substantially. For a detailed discussion of this topic, we refer to the feature article by Nothaft et al. [79] in this issue. STM-induced luminescence may focus increasingly on time-resolved experiments. Here, limitations in todays experimental designs can be identified, as e.g. the non-radiative quenching by the close-by metal electrodes and the plasmonic background emission. When the position of charge carrier recombination cannot be pinned simply by the STM tip position, specific sites may be provided in a heterogeneous structure of the organic layer. This successful concept established by photoluminescence studies has recently been exploited also for the electronic control of single molecule luminescence [80]. The isolation of individual emitters within an organic semiconductor may be transferred to ultrathin film studies. Interestingly, a number of quite similar challenges as the ones listed here were faced in the development of OLEDs [81]. This fact may lead to some similar solutions as e.g. the design of sandwich systems.

Acknowledgements This project was supported by the Deutsche Forschungsgemeinschaft (DFG) via research group FOR 730 “Positioning of single nanostructures – single quantum devices”.

References

[1] F. Kulzer and M. Orrit, Ann. Rev. Chem. **55**, 585 (2004).
[2] B. Lounis and M. Orrit, Rep. Prog. Phys. **68**, 1129 (2005).
[3] H. Klauk, Chem. Soc. Rev. **39**, 2643 (2010).
[4] J. Shinar and R. Shinar, J. Phys. D **41**, 133001 (2008).
[5] K. Kuhnke, A. Kabakchiev, W. Stiepany, F. Zinser, R. Vogelgesang, and K. Kern, Rev. Sci. Instrum. **81**, 113102 (2010).
[6] J. K. Gimzewski, B. Reihl, J. H. Coombs, and R. R. Schlittler, Z. Phys. B **72**, 497 (1988).
[7] S. Ushioda, J. Lumin. **47**, 47 (1991).
[8] R. Berndt and J. K. Gimzewski, Phys. Rev. B **48**, 4746 (1993).
[9] R. Berndt and J. K. Gimzewski, Surf. Sci. **269–270**, 556 (1992).
[10] R. Berndt, R. Gaisch, J. K. Gimzewski, B. Reihl, R. R. Schlittler, W. D. Schneider, and M. Tschudy, Science **262**, 1425 (1993).
[11] R. Berndt, R. Gaisch, W. D. Schneider, J. K. Girazewski, B. Reihl, R. R. Schlittler, and M. Tschudy, Surf. Sci. **307–309**, 1033 (1994).
[12] R. Berndt, R. Gaisch, W. D. Schneider, J. K. Gimzewski, B. Reihl, R. R. Schlittler, and M. Tschudy, Phys. Rev. Lett. **74**, 102 (1995).
[13] Y. Uehara, T. Fujita, and S. Ushioda, Phys. Rev. Lett. **83**, 2445 (1999).
[14] M. Reinhardt, G. Schull, P. Ebert, and R. Berndt, Appl. Phys. Lett. **96**, (2010).
[15] B. N. J. Persson and A. Baratoff, Phys. Rev. Lett. **68**, 3224 (1992).
[16] P. Johansson, R. Monreal, and P. Apell, Phys. Rev. B **42**, 9210 (1990).
[17] J. Aizpurua, G. Hoffmann, S. P. Apell, and R. Berndt, Phys. Rev. Lett. **89**, 156803 (2002).
[18] R. Berndt and J. K. Gimzewski, Phys. Rev. B **45**, 14095 (1992).
[19] L. Samuelson, A. Gustafsson, J. Lindahl, L. Montelius, M. E. Pistol, J. O. Malm, G. Vermeire, and P. Demeester, J. Vac. Sci. Technol. B **12**, 2521 (1994).
[20] S. Ushioda, T. Tsuruoka, Y. Ohizumi, and H. Hashimoto, Braz. J. Phys. **34**, 547 (2004).
[21] X. H. Qiu, G. V. Nazin, and W. Ho, Science **299**, 542 (2003).
[22] S. W. Wu, G. V. Nazin, and W. Ho, Phys. Rev. B **77**, 205430 (2008).
[23] C. Chen, P. Chu, C. A. Bobisch, D. L. Mills, and W. Ho, Phys. Rev. Lett. **105**, 217402 (2010).
[24] R. Berndt, R. Gaisch, W. D. Schneider, J. K. Gimzewski, B. Reihl, R. R. Schlittler, and M. Tschudy, Appl. Phys. A **57**, 513 (1993).
[25] E. Ćavar, M.-C. Blüm, M. Pivetta, F. Patthey, M. Chergui, and W.-D. Schneider, Phys. Rev. Lett. **95**, 196102 (2005).
[26] F. Rossel, M. Pivetta, F. Patthey, and W.-D. Schneider, Opt. Express **17**, 2714 (2009).
[27] Z. C. Dong, X. L. Guo, A. S. Trifonov, P. S. Dorozhkin, K. Miki, K. Kimura, S. Yokoyama, and S. Mashiko, Phys. Rev. Lett. **92**, 086801 (2004).
[28] X. L. Guo, Z. C. Dong, A. S. Trifonov, K. Miki, Y. Wakayama, D. Fujita, K. Kimura, S. Yokoyama, and S. Mashiko, Phys. Rev. B **70**, 233204 (2004).
[29] A. Kabakchiev, K. Kuhnke, T. Lutz, and K. Kern, Chem. Phys. Chem. **11**, 3412 (2010).
[30] F. Rossel, M. Pivetta, F. Patthey, E. Cavar, A. P. Seitsonen, and W.-D. Schneider, Phys. Rev. B **84**, 075426 (2011).
[31] A. S. Davydov and E. F. Sheka, Phys. Status Solidi **11**, 877 (1965).
[32] F. Rossel, M. Pivetta, and W.-D. Schneider, Surf. Sci. Rep. **65**, 129 (2010).
[33] J. Aizpurua, S. P. Apell, and R. Berndt, Phys. Rev. B **62**, 2065 (2000).
[34] N. L. Schneider, G. Schull, and R. Berndt, Phys. Rev. Lett. **105**, 026601 (2010).
[35] J. A. Porto, P. Johansson, S. P. Apell, and T. Lopez-Rios, Phys. Rev. B **67**, 085409 (2003).
[36] Y. Zhang, F. Geng, Y. Gao, Y. Liao, Z. C. Dong, and J. G. Hou, Appl. Phys. Lett. **97**, 243101 (2010).
[37] X. Tao, Z. C. Dong, J. L. Yang, Y. Luo, J. G. Hou, and J. Aizpurua, J. Chem. Phys. **130**, (2009).
[38] G. E. Poirier, Phys. Rev. Lett. **86**, 83 (2001).
[39] H. W. Liu, Y. Ie, R. Nishitani, T. Z. Han, Y. Aso, and H. Iwasaki, Thin Solid Films **516**, 2727 (2008).
[40] H. W. Liu, R. Nishitani, T. Z. Han, Y. Ie, Y. Aso, and H. Iwasaki, Phys. Rev. B **79**, 125415 (2009).

[41] Z. C. Dong, X. L. Zhang, H. Y. Gao, Y. Luo, C. Zhang, L. G. Chen, R. Zhang, X. Tao, Y. Zhang, J. L. Yang, and J. G. Hou, Nature Photon. **4**, 50 (2010).

[42] R. Nishitani, M. Tobaru, A. Kasuya, H. Liu, and H. Iwasaki, Jpn. J. Appl. Phys. **45**, L627 (2006).

[43] H. W. Liu, Y. Ie, R. Nishitani, Y. Aso, and H. Iwasaki, Phys. Rev. B **75**, 115429 (2007).

[44] T. Basché, W. E. Moerner, M. Orrit, and H. Talon, Phys. Rev. Lett. **69**, 1516 (1992).

[45] M. Orrit, Single Mol. **3**, 255 (2002).

[46] P. Michler, A. Imamoglu, M. D. Mason, P. J. Carson, G. F. Strouse, and S. K. Buratto, Nature **406**, 968 (2000).

[47] F. Silly and F. Charra, Appl. Phys. Lett. **77**, 3648 (2000).

[48] K. Perronet, G. Schull, P. Raimond, and F. Charra, Europhys. Lett. **74**, 313 (2006).

[49] H. Klauk, M. Halik, U. Zschieschang, G. Schmid, W. Radlik, and W. Weber, J. Appl. Phys. **92**, 5259 (2002).

[50] C. C. Mattheus, A. B. Dros, J. Baas, A. Meetsma, J. Ld. Boer, and T. T. M. Palstra, Acta Crystallogr. **C57**, (2001).

[51] C. D. Dimitrakopoulos, A. R. Brown, and A. Pomp, J. Appl. Phys. **80**, 2501 (1996).

[52] L. Ruppel, A. Birkner, G. Witte, C. Busse, T. Lindner, G. Paasch, and C. Woll, J. Appl. Phys. **102**, 033708 (2007).

[53] D. Nabok, P. Puschnig, C. Ambrosch-Draxl, O. Werzer, R. Resel, and D.-M. Smilgies, Phys. Rev. B **76**, 235322 (2007).

[54] S. Seo and P. G. Evans, J. Appl. Phys. **106**, 103521 (2009).

[55] E. Heinecke, D. Hartmann, and A. Hese, J. Chem. Phys. **118**, 113 (2003).

[56] M. Hartmann, A. Lindinger, P. Toennies, and A. F. Vilesov, Chem. Phys. **239**, 139 (1998).

[57] W. E. Geacintov, J. Burgos, I. M. Pope, and C. Strom, Chem. Phys. Lett. **11**, 504 (1971).

[58] A. F. Prikhotko, A. F. Skorobogatko, and L. I. Tsikora, Opt. Spectrosc. **26**, 115 (1969).

[59] U. P. Wild, F. Guttler, M. Pirotta, and A. Renn, Chem. Phys. Lett. **193**, 451 (1992).

[60] R. He, X. Chi, A. Pinczuk, D. V. Lang, and A. P. Ramirez, Appl. Phys. Lett. **87**, 211117 (2005).

[61] R. He, N. G. Tassi, G. B. Blanchet, and A. Pinczuk, Appl. Phys. Lett. **87**, 103107 (2005).

[62] T. Aoki-Matsumoto, K. Furuta, T. Yamada, H. Moriya, and K. Mizuno, Int. J. Mod. Phys. B **15**, 3753 (2001).

[63] H. Marciniak, I. Pugliese, B. Nickel, and S. Lochbrunner, Phys. Rev. B **79**, 235318 (2009).

[64] T. Lutz, A. Kabakchiev, T. Dufaux, C. Wolpert, Z. Wang, M. Burghard, K. Kuhnke, and K. Kern, Small **7**, 2396 (2011).

[65] U. Heinemeyer, K. Broch, A. Hinderhofer, M. Kytka, R. Scholz, A. Gerlach, and F. Schreiber, Phys. Rev. Lett. **104**, 257401 (2010).

[66] P. Bordat, M. Orrit, R. Brown, and A. Würger, Chem. Phys. **258**, 63 (2000).

[67] R. B. Campbell, J. M. Robertson, and J. Trotter, Acta Crystallogr. **14**, 705 (1961).

[68] K. Kuhnke, A. Kabakchiev, T. Lutz, and K. Kern, in preparation (2012).

[69] Single photon counting module SPCM-AQRH-14, supplier: Perkin–Elmer, USA.

[70] Time correlated single photon counting PC card SPC-130, supplier: Becker&Hickl, Germany.

[71] C. Kurtsiefer, P. Zarda, S. Mayer, and H. Weinfurter, J. Mod. Opt. **48**, 2039 (2001).

[72] H. Marciniak, M. Fiebig, M. Huth, S. Schiefer, B. Nickel, F. Selmaier, and S. Lochbrunner, Phys. Rev. Lett. **99**, 176402 (2007).

[73] B. N. J. Persson and N. D. Lang, Phys. Rev. B **26**, 5409 (1982).

[74] F. Balzer, V. G. Bordo, and H.-G. Rubahn, Opt. Lett. **22**, 1262 (1997).

[75] K. Kuhnke, R. Becker, M. Epple, and K. Kern, Phys. Rev. Lett. **79**, 3246 (1997).

[76] D. Faltermeier, B. Gompf, M. Dressel, A. K. Tripathi, and J. Pflaum, Phys. Rev. B **74**, 125416 (2006).

[77] G. Tian, J.-C. Liu, and Y. Luo, Phys. Rev. Lett. **106**, 177401 (2011).

[78] S. Berkebile, P. Puschnig, G. Koller, M. Oehzelt, F. P. Netzer, C. Ambrosch-Draxl, and M. G. Ramsey, Phys. Rev. B **77**, 115312 (2008).

[79] M. Nothaft, S. Höhla, F. Jelezko, J. Pflaum, and J. Wrachtrup, Phys. Status Solidi B **249**, 653 (2012), this issue.

[80] M. Nothaft, S. Höhla, A. Nicolet, F. Jelezko, N. Frühauf, J. Pflaum, and J. Wrachtrup, Chem. Phys. Chem. **12**, 2590 (2011).

[81] N. K. Patel, S. Cinà, and J. H. Burroughes, IEEE J. Sel. Top. Quantum Electron. **8**, 346 (2002).